# Effect of Target Gas Temperature on the Scattering Cross Section*

ARNOLD RUSSEK
*Department of Physics, University of Connecticut, Storrs, Connecticut*
(Received April 25, 1960)

If a beam of particles is scattered by a gas or plasma, the differential scattering cross section that is observed experimentally may, in some cases, be altered a discernible amount by the random thermal motion of the target particles. In order to explore the feasibility of using this effect as a means of measuring high temperatures, or to correct for the temperature of the target in the event that the desired cross section must be measured at high temperatures, this work presents a theoretical study of the temperature dependence of the cross section. A general expression is obtained for the observed differential scattering cross section in the laboratory frame in terms of the differential cross section in the center-of-mass frame for the general case of arbitrary initial motion of the target. Detailed results for the temperature dependence are given for hard-sphere scattering (which is also applicable to low-energy neutron scattering) and for Coulomb scattering, in the approximation in which the projectiles are light and rapidly moving, compared to the targets. For hard-sphere scattering the case of equal projectile and target mass is also considered.

## 1. INTRODUCTION

IN ordinary scattering phenomena, the thermal motion of the scattering centers can usually be neglected, in comparison with the much larger velocity of the incident beam projectiles. This is quite fortunate, inasmuch as scattering experiments are usually used to determine the physical properties of one or the other colliding particles, or to study the interaction between the two, and it would be much more difficult to extract the desired information from the data, were there an additional set of random variables (speeds and directions of the targets) to complicate the initial conditions.

However, in some cases, it may be necessary to conduct the scattering experiment with the target at relatively high temperatures. As an example, if it is desired to study the collisions of various projectiles with atomic hydrogen as the target, the target gas of pressure, perhaps a micron, would have to be maintained at 2400°K in order to insure that it is fully dissociated. For low-energy projectiles, the temperature effect might well be appreciable. At any rate, it would certainly be desirable to know, in advance, the order of magnitude of the effect and to be able to correct the data where necessary. A second example is the scattering of low-energy neutrons by protons, an experiment which has, in fact, been conducted.[1]

There is also an additional, and perhaps more important reason for studying the temperature dependence of the observed differential scattering cross section. The possibility exists that a suitable beam of particles at the proper energy could be used as a probe to measure the temperature and density of a gas or plasma as a function of position. Thus, if the differential scattering cross section is known in the center-of-mass system, for given projectile and target, two families of curves can be computed giving the number of particles scattered per unit solid angle as a function of angle of scattering, with target gas temperature and density as parameters. With these, the temperature and density of the target gas at a given point can be obtained by measuring and plotting this quantity and comparing the measured curve with the two families of computed curves.

At sufficiently low densities, the density dependence of the number of particles scattered per unit solid angle is such that the shape of the curve, plotted as a function of angle, remains unchanged, with only the ordinate scale factor varying. In contrast to this, the primary effect of a change in temperature is to alter the shape of the curve without much changing the average height. Thus, even if only the temperature is desired, measurements at at least two angles are necessary, in order that lack of precise knowledge of the density shall not cause an incorrect temperature determination.

Of course, the practical utility of this method of measuring temperature depends on the sensitivity of the differential cross-section curve to a change in target gas temperature. The method will, in any event, be relatively cumbersome, but this disadvantage is offset by the advantages that (1) the technique may be feasible at the very high temperatures where other methods fail and (2) it can be made to give instantaneous temperature readings as a function of position, and might, therefore, become an important tool for studying nonequilibrium phenomena. Figure 1 shows how the collimation of the incident and scattered

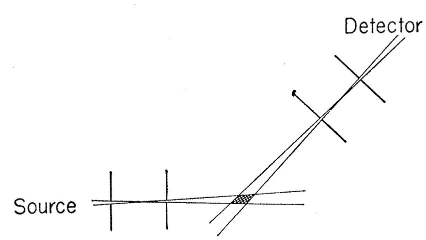


FIG. 1. Geometrical arrangement. This shows how collimation of the incident and scattered beams selects a small region of observation.

* This work was supported by the Office of Ordnance Research, U. S. Army, through the Ordnance Materials Research Office at Watertown and the Boston Ordnance District.

[1] W. B. Jones, Jr., Phys. Rev. 74, 364 (1948).

beams selects a very small region of observation. To obtain instantaneous temperature determinations, it is, of course, necessary to measure the scattered beam intensity at several angles simultaneously. The speed of the temperature determination would essentially be limited by the admissible intensity of the incident beam in relation to the size of the cross section, the target density, and the sensitivity or efficiency of the detector.

The purpose of the present study is to determine theoretically the dependence of the target gas temperature in terms of the (presumed known) cross section in the center-of-mass frame. Gryzinski,[2] Chandrasekhar[3] and Chandrasekhar and Williamson[4] have considered scattering problems in which the targets were randomly moving with non-negligible velocities, but all three of the above treatments were restricted to Rutherford-type scattering and did not obtain the temperature dependence of the differential scattering cross section.

In the following section a general expression is derived for the quantity $\sigma(T,\theta)$, which gives the observed differential scattering cross section in the laboratory system as a function of target gas temperature, in terms of the differential scattering cross section in the center-of-mass frame. This result is rather complicated. Therefore, in Sec. 3, the approximation for light projectiles incident on slowly moving targets is considered. This case is a good approximation to the scattering of moderate energy electrons, protons, or neutrons by most gases at any temperature that would be of interest. Two special cases, Rutherford and hard-sphere scattering, are considered in detail. The latter case is also applicable to the elastic scattering of low-energy neutrons. Inasmuch as scattering experiments with low-energy neutrons incident on protons have already been performed, the special case of target mass equal to projectile mass is considered for this type of collision.

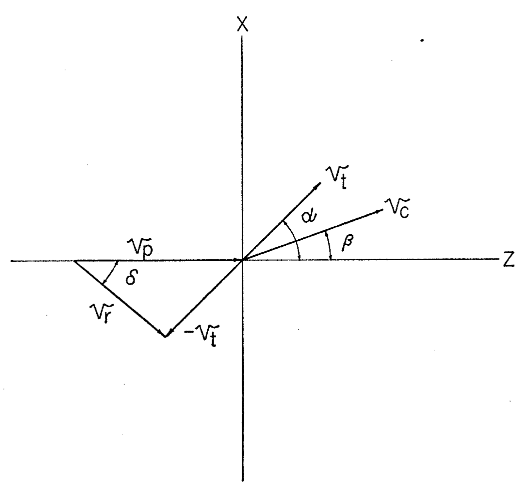


FIG. 2. A velocity diagram in the laboratory frame. Here $\mathbf{v}_c$ is the velocity of the center of mass, $\mathbf{v}_t$ the velocity of the target, $\mathbf{v}_r$ the relative velocity.

[2] M. Gryzinski, Phys. Rev. **115**, 374 (1959).
[3] S. Chandrasekhar, Astrophys. J. **93**, 285 (1941).
[4] S. Chandrasekhar and R. E. Williamson, Astrophys. J. **93**, 308 (1941).

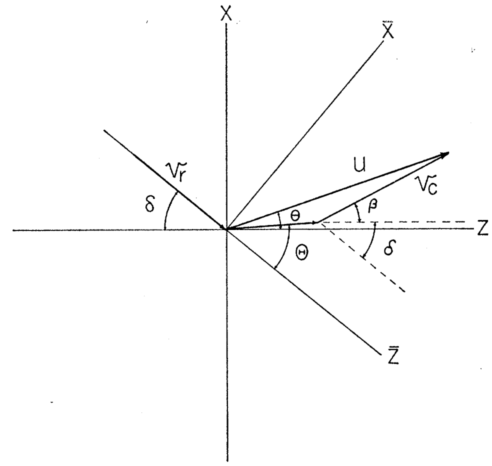


FIG. 3. Relation between the angle of scattering $\theta$ in the laboratory frame and the angle of scattering $\Theta$ in the center-of-mass frame. In order not to complicate the figure, this shows the special case in which $\Phi=0$, but the analysis in the text is perfectly general.

Section 4 presents some numerical results and conclusions drawn from the analysis.

## 2. GENERAL FORMULATION

For a gas at sufficiently low densities so that multiple scattering can be neglected, we denote by $\sigma(T,\theta)$ the number of particles scattered per unit time, in the laboratory system, into a unit solid angle making an angle $\theta$ with the incident direction per target particle for unit intensity beam. This is the usual definition, but we are here taking formal cognizance of the fact that $\sigma$ is a function of the target gas temperature $T$. In most applications the $T=0$ isotherm is understood.

In order to calculate $\sigma(T,\theta)$, let us first consider the scattering produced by a target moving with velocity $\mathbf{v}_t$, in a direction making an angle $\alpha$ with the direction of motion of the incident projectile. We choose a coordinate system such that the projectile is traveling in the positive $z$ direction and the target is moving in the $x$-$z$ plane (see Fig. 2). We take it for granted that the cross section in the center-of-mass frame, $\sigma_c(\Theta)$ is known. (It is independent of azimuthal angle $\Phi$ for central forces.) Here $\Theta$, $\Phi$ give the scattered direction in the $\bar{X}$, $\bar{Y}$, $\bar{Z}$ coordinate system of the center-of-mass frame (see Fig. 3). Also, $\delta$ gives the angle that the relative velocity $\mathbf{v}_r$ makes with respect to the $z$ axis, $v_c$ and $\beta$ are, respectively, the speed and direction of motion of the center-of-mass in the laboratory system. Finally, $u$, $\theta$, $\varphi$ represent the final speed and direction of motion of the projectile, in the $x$, $y$, $z$ coordinate system fixed in the laboratory frame (see Fig. 3). In order not to clutter Fig. 3, it shows only the special case $\Phi=0$, but the analysis below and in the Appendix is completely general.

If, in the center-of-mass frame, the projectile is scattered into the direction $\Theta$, $\Phi$, it is possible to solve for the angles $\theta$, $\varphi$ describing the direction of scattering in the laboratory frame of reference. Thus:

$$\begin{aligned}\Theta&=\Theta(\theta,\varphi,\alpha),\\ \Phi&=\Phi(\theta,\varphi,\alpha),\end{aligned} \tag{1}$$

where we suppress explicit mention of the dependence of $\Theta$ and $\Phi$ on $v_p$ and $v_t$, since these will remain unchanged in the operations performed below.

To obtain the cross section in the laboratory frame, $\sigma_\alpha(\theta,\varphi)$, in terms of the cross section in the center-of-mass frame, the connection is given by

$$\sigma_c(\Theta)\sin\Theta d\Theta d\Phi=\sigma_\alpha(\theta,\varphi)\sin\theta d\theta d\varphi. \tag{2}$$

Since

$$d\Theta d\Phi=J\begin{pmatrix}\Theta, & \Phi\\ \theta, & \varphi\end{pmatrix}d\theta d\varphi, \tag{3}$$

where $J$ is the Jacobian of the transformation (1), we have

$$\sigma_\alpha(\theta,\varphi)=\frac{\sin\Theta}{\sin\theta}J\begin{pmatrix}\Theta, & \Phi\\ \theta, & \varphi\end{pmatrix}\sigma_c(\Theta). \tag{4}$$

Now, $\sigma_\alpha$ is the cross section, in the laboratory frame, for the special case in which the target is moving in a direction which makes an angle $\alpha$ with respect to the direction of motion of the projectile. No azimuthal angle is used since we have chosen our coordinate system such that the target is moving in the $x$-$z$ plane.

The desired cross section is obtained by averaging $\sigma_\alpha$ over all directions and speeds of the targets. Insofar as the azimuthal angle is concerned, this can be accomplished by averaging over all orientations of the $x$ axis about the $z$ axis, i.e., integrating over $\varphi$ and dividing by $2\pi$. Averaging over $\alpha$ and $v_t$ is straightforward. Thus:

$$\sigma(T,\theta)=\int_0^\infty f(v_t)dv_t\int_0^\pi \tfrac{1}{2}\sin\alpha d\alpha \times\int_0^{2\pi}\frac{1}{2\pi}d\varphi\left[\frac{\sin\Theta}{\sin\theta}J\begin{pmatrix}\Theta, & \Phi\\ \theta, & \varphi\end{pmatrix}\sigma_c(\Theta)\right]. \tag{5}$$

Here, $f(v_t)$ is the distribution function of the speeds and it must be remembered that the quantity in square brackets is a function of $v_t$. In order to formally exhibit $\sigma$ as a function of temperature, the function in the square brackets would have to be expanded as a power series in $v_t$ and the various moments of $v_t$ expressed in terms of $T$. This will be done in the following sections.

It is shown in the Appendix that

$$\frac{\sin\Theta}{\sin\theta}J\begin{pmatrix}\Theta, & \Phi\\ \theta, & \varphi\end{pmatrix}=\frac{u^2}{V_p[V_p^2+v_c^2(A^2-1)]^{\frac{1}{2}}}, \tag{6}$$

with

$$V_p=v_p(1+\eta)^{-1}(1-2\xi\cos\alpha+\xi^2)^{\frac{1}{2}}, \tag{7a}$$

$$v_c=v_p(1+\eta)^{-1}(\eta^2+2\xi\eta\cos\alpha+\xi^2)^{\frac{1}{2}}, \tag{7b}$$

$$A=(\eta^2+2\xi\eta\cos\alpha+\xi^2)^{-\frac{1}{2}} \times[\xi(\sin\theta\cos\varphi\sin\alpha+\cos\theta\cos\alpha)+\eta\cos\theta], \tag{7c}$$

$$u=Av_c+[V_p^2+v_c^2(A^2-1)]^{\frac{1}{2}}, \tag{7d}$$

where

$$\xi=v_t/v_p,\quad \eta=m_p/m_t. \tag{7e}$$

The quantities defined in Eqs. (7a-d) have physical significance. Thus, $V_p$ is the velocity of the projectile in the center-of-mass frame; $v_c$ is the speed of the center-of-mass in the laboratory frame; $A$ is the cosine of the angle between the final projectile velocity and the velocity of the center-of-mass, both being measured in the laboratory frame; finally, $u$ is the final projectile speed in the laboratory frame. The particular choice of the dimensionless quantities $\xi$ and $\eta$, defined in (7e), is dictated by the fact that for slowly moving targets and light projectiles, $\xi$ and $\eta$ will be small, and it is this case that is next considered in detail.

## 3. SLOWLY MOVING TARGETS

### A. Light Projectiles

In the case of light projectiles and slowly moving targets, $\eta$ and $\xi$ are small. A Taylor expansion of the right-hand side of Eq. (6) with only the first few terms retained will then yield a good approximation. It is necessary to carry out the expansions to order $\xi^2$, since the contribution of the terms linear in $\xi$ to the differential cross section vanishes. Carrying out the expansion is straightforward, but tedious. The result is given in Eqs. (8).

$$\begin{aligned}\frac{\sin\Theta}{\sin\theta}J\begin{pmatrix}\Theta, & \Phi\\ \theta, & \varphi\end{pmatrix}&=K_0+\xi[K_{1c}\cos\alpha+K_{1s}\sin\alpha\cos\varphi]+\xi^2[K_{2cc}\cos^2\alpha\\ &\quad+(K_{2ss}^{(c)}\cos^2\varphi+K_{2ss}^{(s)}\sin^2\varphi)\sin^2\alpha\\ &\quad+K_{2sc}\sin\alpha\cos\alpha]+\cdots,\end{aligned} \tag{8a}$$

which explicitly exhibits the dependence on $\xi$, $\alpha$, and $\varphi$. Here,

$$K_0=1+\eta 2\cos\theta+\eta^2(1/2)(3\cos^2\theta-1)+\cdots, \tag{8b}$$

$$K_{1c}=2\cos\theta+\eta(3\cos^2\theta+2\cos\theta-1)+\cdots, \tag{8c}$$

$$K_{1s}=2\sin\theta+\eta 3\sin\theta\cos\theta+\cdots, \tag{8d}$$

$$K_{2cc}=(1/2)(3\cos^2\theta+4\cos\theta-1) +\eta 2(3\cos^2\theta+\cos\theta-1)+\cdots, \tag{8e}$$

$$K_{2ss}^{(c)}=(1/2)(-3\cos^2\theta+2)-\eta\cos\theta+\cdots, \tag{8f}$$

$$K_{2ss}^{(s)}=-1/2-\eta\cos\theta+\cdots. \tag{8g}$$

$K_{2sc}$ is not needed. The contribution of that term to the cross section will vanish to order $\xi^2$ because of the $\alpha$ and $\varphi$ dependence. The coefficient of each power of $\xi$ is given as a power series in $\eta$, with only the first two terms retained (except that in the expansion of the coefficient of $\xi^0$, the first three terms are retained). This somewhat strange presentation of the series expansion of $J\sin\Theta/\sin\theta$ is motivated by the fact that it is necessary to go to order $\xi^2$ to get a nonvanishing correction to the cross section. This is shown in paragraph $C$ of this section. It is moreover necessary to go to order $\xi^2\eta$ to get an indication of the mass ratio dependence of that correction. Terms, therefore, of order $\xi\eta^2$, which are of the same order have not been retained, since they do not contribute to the cross section.

### 1. Hard-Sphere Collisions

Let the radii of projectile and target be denoted by $R_p$ and $R_t$; then[5]

$$\sigma_c = a^2 \quad a=(R_p+R_t)/2. \tag{9}$$

This cross section is also valid for elastic scattering of neutrons at low energies.[6] In that case, $a$ is known as the "scattering length."

Substitution of Eq. (9) along with Eqs. (8) into Eq. (5), and then carrying out the indicated integrations yields:

$$\sigma(T,\theta)=a^2\{[1+2\eta\cos\theta+\eta^2\tfrac{1}{2}(3\cos^2\theta-1)+\cdots] + (\eta kT/E_p)[\cos\theta+\eta(3\cos^2\theta-1)+\cdots] +\cdots\}, \tag{10}$$

where $E_p$ is the energy of the projectile in the laboratory frame. In deriving the result (10), the usual definition of $T$ is used:

$$\int_0^\infty f(v_t)\xi^2 dv_t = \int_0^\infty f(v_t)\frac{v_t^2}{v_p^2}dv_t = \frac{3kT}{m_t v_p^2} = \frac{3kT\eta}{2E_p}. \tag{11}$$

The first moment of $\xi$ is not needed, since, as mentioned before, the terms linear in $\xi$ vanish upon integration over the angles. It should not be inferred from Eq. (10) that, in the limit $\eta\to 0$ the temperature-dependent term vanishes, since $E_p$ also goes to zero. The ratio $\eta kT/E_p$ remains finite and is equal to $2kT/m_t v_p^2$.

Integrating over all solid angles to find the total cross section, we find that all terms in $\eta$ and $T$ drop out, leaving

$$\sigma_{\text{tot}} = 4\pi a^2, \tag{12}$$

which is the same result as is obtained for initially motionless targets: $T=0$. This is not surprising, inasmuch as the motion of a target cannot affect the total area it presents for collision; it only affects the distribution in angles of scattering of those collisions that do occur.

[5] See, e.g., R. D. Present, *Kinetic Theory of Gases* (McGraw-Hill Book Company, Inc., New York, 1958), pp. 140–142.

[6] J. M. Blatt and V. F. Weisskopf, *Theoretical Nuclear Physics* (John Wiley & Sons, New York, 1952), pp. 56–65.

### 2. Coulomb Scattering

Here,

$$\sigma_c(\Theta)=\frac{(Z_pZ_te^2)^2}{m_p^2V_p^4}\frac{1}{(1-\cos\Theta)^2}$$
$$=\Sigma_0+\xi[\Sigma_{1c}\cos\alpha+\Sigma_{1s}\cos\varphi\sin\alpha] +\xi[\Sigma_{2cc}\cos^2\alpha+\Sigma_{2ss}\cos^2\varphi\sin^2\alpha +\Sigma_{2sc}\cos\varphi\sin\alpha\cos\alpha], \tag{13a}$$

where

$$\Sigma_0=S[1-\eta 2(1+\cos\theta) +\eta^2(2\cos^2\theta+5\cos\theta+3)], \tag{13b}$$

$$\Sigma_{1c}=S[2(1-\cos\theta)+\eta 4(\cos^2\theta-1)], \tag{13c}$$

$$\Sigma_{1s}=S[-2\sin\theta+\eta\sin\theta(4\cos\theta+6)], \tag{13d}$$

$$\Sigma_{2cc}=S[2\cos^2\theta-5\cos\theta+3-\eta 3(1+\cos\theta) \times(\cos^2\theta-3\cos\theta+2)], \tag{13e}$$

$$\Sigma_{2ss}=S[1-\cos\theta-2\cos^2\theta +\eta(1+\cos\theta)(3\cos^2\theta+7\cos\theta-6)], \tag{13f}$$

$$S=(Z_pZ_te^2)^2(1+\eta)^4/m_p^2v_p^4(1-\cos\theta)^2. \tag{13g}$$

$\Sigma_{2sc}$ is not needed, since it does not contribute to the cross section. Substitution of Eqs. (13) along with Eqs. (8) into Eq. (5) and carrying out the indicated integrations yields, upon simplification of the final result:

$$\sigma(\theta,T)=S\{[1-2\eta+(1/2)\eta^2(5+2\cos\theta-\cos^2\theta)] -(2\eta^2kT/E_p)(1-\cos\theta)^2\}. \tag{14}$$

Again, Eq. (11) was used to express the second moment of $v_t$ in terms of target gas temperature.

### 3. The General Case

The general case can be treated by expressing $\sigma_c(v_p,\Theta)$ as a function of $V_p$ and $\cos\Theta$,

$$\sigma_c = f(V_p, \cos\Theta), \tag{15}$$

and then substituting for $V_p$ the expression given by Eq. (7a) and for $\cos\Theta$ from Eq. (24c) of the Appendix. It is instructive to expand this as a power series in $V_p$ and $\cos\Theta$,

$$\sigma_c=\sum_{n,m} A_{nm}V_p^n\cos^m\Theta, \tag{16}$$

and to expand the expressions (7a) and (24c) for $V_p$ and $\cos\Theta$ in terms of $\xi$ and $\eta$:

$$V_p=v_p(1+\eta)^{-1}(1-\xi\cos\alpha+\xi^2\tfrac{1}{2}\sin^2\alpha+\cdots), \tag{17a}$$

$$\cos\Theta=c_0+\xi[c_{1c}\cos\alpha+c_{1s}\sin\alpha\cos\varphi] +\xi^2[c_{2cc}\cos^2\alpha+c_{2ss}\sin^2\alpha+c_{2sc}\sin\alpha\cos\alpha], \tag{17b}$$

where

$$c_0=\cos\theta-\eta\sin^2\theta-\tfrac{1}{2}\eta^2\sin^2\theta\cos\theta+\cdots, \tag{17c}$$

$$c_{1c}=-\sin^2\theta[1+\eta(1+\cos\theta)+\cdots], \tag{17d}$$

$$c_{1s}=\sin\theta(\cos\theta-1)[1+\eta\cos\theta+\cdots], \tag{17e}$$

$$c_{2cc}=-\sin^2\theta[(1+\tfrac{1}{2}\cos\theta)+\eta(2\cos\theta+1)+\cdots], \tag{17f}$$

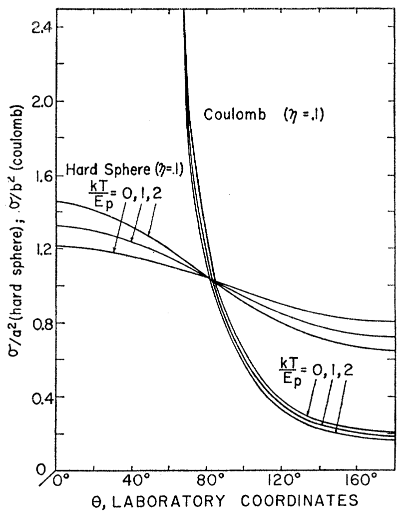


FIG. 4. Temperature dependence of the differential scattering cross section for hard-sphere scattering and for Coulomb scattering. Here $a$ is defined in Eq. (9) and $b=Z_pZ_te^2(1+\eta)^2/m_pv_p^2$.

$$c_{2ss}=(\cos\theta-1)[(-\sin^2\varphi+\tfrac{1}{2}\cos\theta(1-\cos\theta)\cos^2\varphi)+\eta\cos\theta(\cos\theta+1)\cos^2\varphi+\cdots]. \quad (17g)$$

The coefficient $c_{2sc}$ is not needed. It will be noted from Eqs. (17) that the coefficients of $\xi^0$ in both $V_p$ and $\cos\Theta$ are independent of both $\alpha$ and $\varphi$. Moreover, the coefficients of $\xi^1$ vary as $\cos\alpha$ and $\sin\alpha\cos\varphi$. It then follows that the terms linear in $\xi$ in both $V_p{}^n$ and $\cos^m\Theta$ and, therefore, in the product $V_p{}^n\cos^m\Theta$ will be a combination of $\cos\alpha$ and $\sin\alpha\cos\varphi$ (multiplied by things independent of $\alpha$ and $\varphi$). It will be further noted from Eqs. (8) that the terms in $\xi^0$ and $\xi^1$ in $J\sin\Theta/\sin\theta$ have similar dependences on $\alpha$ and $\varphi$. As a consequence, the expansion of the integrand in Eq. (5) has the form $f_1(\theta,\eta)+\xi[f_2(\theta,\eta)\cos\alpha+f_3(\theta,\eta)\sin\alpha\cos\varphi]$ plus higher order terms. Upon integration over $\alpha$ and $\varphi$, the second term vanishes, leaving the first term unaltered (the zero-temperature result) plus terms in $\xi^2$ which give a correction linear in $T$.

### B. Projectile Mass Equals Target Mass

The case in which $\eta=1$ will also be considered for hard-sphere scattering, since this result is applicable to the scattering of low-energy neutrons by protons. In this case, the expansion of (6) and its subsequent substitution, along with $\sigma_c(\Theta)$ given by (9), into Eq. (5) yields:

$$\sigma(T,\theta)=4\cos\theta[1+(kT/2E_p)(1+\cos^{-4}\theta)]. \quad (18)$$

This result is not valid near $\theta=\pi/2$.

## 4. NUMERICAL RESULTS AND CONCLUSIONS

Figure 4 presents some numerical results, computed from Eq. (10) for hard-sphere scattering and from Eq. (14) for Coulomb scattering, for the case in which the mass of the projectile is one tenth that of the target. The differential cross section is plotted as a function of angle with target gas temperature as a parameter. It is seen that for light projectiles, Coulomb scattering is quite insensitive to the temperature. As a matter of fact, it can be seen from Eq. (14) that in the limit $\eta\to 0$, the temperature-dependent term vanishes entirely. On the other hand, hard-sphere scattering (which describes the elastic scattering of low-energy neutrons) exhibits a much more detectable temperature dependence. It should not be immediately concluded from Fig. 4 that a neutron beam is always a more sensitive probe of temperature than a proton beam. The cross section for low-energy protons on neutral atoms is of the shielded Coulomb type, which should behave more like the hard-sphere case than the simple Coulomb case. However, at the high temperatures at which one would consider using this method, the target gas atoms would most certainly be at least partially ionized and would give rise to Coulomb-type scattering even at low projectile energy. Consequently, the remaining calculations all deal exclusively with hard-sphere scattering.

Figure 5 shows how a measurement of the fraction of projectiles scattered per unit solid angle at two angles 0° and 180° suffice to determine both temperature and particle density. The curves rising to the right

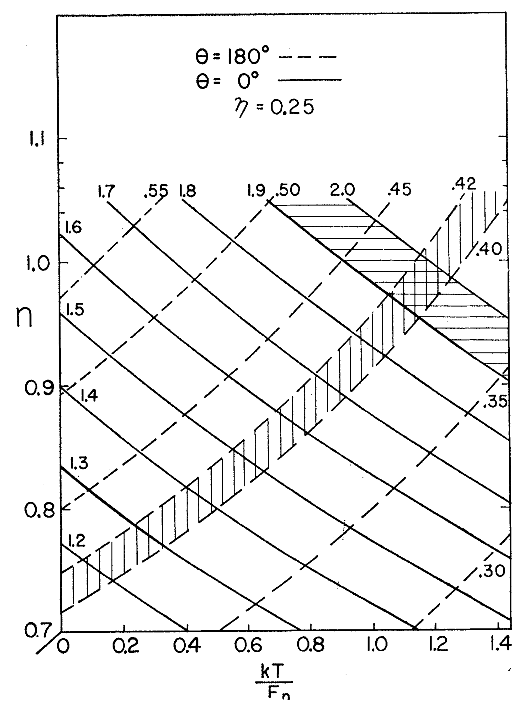


FIG. 5. Diagram illustrating how a measurement of the fraction of the projectiles scattered per unit solid angle at two angles 0° and 180° suffices to determine both temperature (given in dimensionless units along the abscissa) and particle density (given along the ordinate). The solid lines pertain to the measurement at 0°, while the dashed lines pertain to the measurement at 180°. The numbers associated with each of the curves are the values of the quantity $(N_0ta^2)^{-1}dN/d\omega$.

establish the relation between temperature and particle density determined by an experimental determination of $(N_0ta^2)^{-1}\,dN/d\omega$ at angle of scattering of 180° in the laboratory frame. Here, $N_0$ is the number of projectiles incident, $t$ the target gas thickness, $dN/d\omega$ the number of particles scattered per unit solid angle, and $a$ is defined in Eq. (9). Similarly, the curves rising to the left establish another relation obtained by a similar measurement at 0° scattering angle. (In practice, angles of say 5° and 175° would be chosen so as to eliminate interference with the incident beam.) The hatched regions show how such measurements, with an error of 2.5% determine the density with an error of 5% and $kT/E_p$ with an error of 18%. For a target gas at $10^6$ °K, the energy of the incident beam of neutrons required to obtain this accuracy would be 78 ev; on the other hand, a 0.78-ev neutron beam could measure a temperature of $10^4$ °K with the same accuracy.

As a final point, it may be remarked that the experiment reported in reference 1 considered the scattering cross section of neutrons incident on protons at energies of from 0.003 ev to 100 ev. At energies of 0.03 ev and lower, the alteration in the angular dependence of the differential cross section becomes appreciable. Unfortunately, that particular experiment measured only the total cross section, not the angular dependence. It is mentioned here only to illustrate that measurements in a range in which the temperature dependence is important are indeed feasible.

### 5. ACKNOWLEDGMENTS

The author would like to thank Dr. Edgar Everhart for helpful comments on the preparation of the manuscript.

### 6. APPENDIX

The functional dependence of $\Theta$ and $\Phi$ upon $\theta$, $\varphi$, $v_p$, $v_t$ and $\alpha$, indicated in Eq. (1) will now be explicitly determined. In order to avoid confusion, it is best to point out that three coordinate systems are employed: an $\bar{X}$, $\bar{Y}$, $\bar{Z}$ system fixed in the center-of-mass system and both an $\bar{x}$, $\bar{y}$, $\bar{z}$ and an $x$, $y$, $z$ system, each fixed in the laboratory. The two barred systems are moving relative to each other but have parallel coordinate axes. The $x$, $y$, $z$ and $\bar{x}$, $\bar{y}$, $\bar{z}$ systems are merely rotated with respect to each other by the angle $\delta$ in the $x$-$z$ plane.

From Fig. 2, the direction and magnitude of the initial relative velocity is easily determined. This will be denoted by $v_r$.

$$v_r=(v_p^2-2v_pv_t\cos\alpha+v_t^2)^{\frac{1}{2}}=v_p(1-2\xi\cos\alpha+\xi^2)^{\frac{1}{2}}, \quad (19a)$$

$$v_r\sin\delta=v_t\sin\alpha. \quad (19b)$$

The velocity of the projectile in the center-of-mass system, denoted by $V_p$, follows directly from the definition of the center of mass, and is given by

$$V_p=m_tv_r/(m_p+m_t)=v_r/(1+\eta). \quad (20)$$

The final velocity of the projectile will have, in the center-of-mass frame, the same magnitude as before collision, but will have a direction described by the angles $\Theta$, $\Phi$ in the $\bar{X}$, $\bar{Y}$, $\bar{Z}$ system fixed in the center-of-mass frame. The final projectile velocity in the $\bar{x}$, $\bar{y}$, $\bar{z}$ system fixed in the laboratory is then obtained by adding the velocity of the center of mass to this velocity. Now, by the definition of center of mass, the direction and magnitude of its velocity in the laboratory system is determined by

$$(v_c)_x\equiv v_c\sin\beta=v_p(1+\eta)^{-1}\xi\sin\alpha, \quad (21a)$$

$$(v_c)_z\equiv v_c\cos\beta=v_p(1+\eta)^{-1}(\eta+\xi\cos\alpha), \quad (21b)$$

$$v_c=v_p(1+\eta)^{-1}(\eta^2+2\xi\eta\cos\alpha+\xi^2)^{\frac{1}{2}}. \quad (21c)$$

Moreover, from Fig. 3, it is clear that

$$(v_c)_{\bar{x}}=v_c\sin(\beta+\delta), \quad (22a)$$

$$(v_c)_{\bar{y}}=0, \quad (22b)$$

$$(v_c)_{\bar{z}}=v_c\cos(\beta+\delta). \quad (22c)$$

Thus, we obtain the final velocity of the projectile in the $\bar{x}$, $\bar{y}$, $\bar{z}$ coordinate system of the laboratory frame.

$$u_{\bar{x}}=V_p\sin\Theta\cos\Phi+v_c\sin(\beta+\delta), \quad (23a)$$

$$u_{\bar{y}}=V_p\sin\Theta\sin\Phi, \quad (23b)$$

$$u_{\bar{z}}=V_p\cos\Theta+v_c\cos(\beta+\delta). \quad (23c)$$

In order to find $\Theta$ and $\Phi$ in terms of $\theta$ and $\varphi$ we must express the components $u_{\bar{x}}$, $u_{\bar{y}}$, $u_{\bar{z}}$ in the laboratory coordinate system in terms of $u_x$, $u_y$, $u_z$.

$$u_{\bar{x}}=u_x\cos\delta+u_z\sin\delta$$
$$=u(\sin\theta\cos\varphi\cos\delta+\cos\theta\sin\delta), \quad (24a)$$

$$u_{\bar{y}}=u_y=u(\sin\theta\sin\varphi), \quad (24b)$$

$$u_{\bar{z}}=u_z\cos\delta-u_x\sin\delta$$
$$=u(\cos\theta\cos\delta-\sin\theta\cos\varphi\sin\delta). \quad (24c)$$

Substituting (24) into (23) and transposing the terms involving $v_c$:

$$V_p\sin\Theta\cos\Phi=u(\sin\theta\cos\varphi\cos\delta+\cos\theta\sin\delta)$$
$$-v_c\sin(\beta+\delta), \quad (25a)$$

$$V_p\sin\Theta\sin\Phi=u(\sin\theta\sin\varphi), \quad (25b)$$

$$V_p\cos\Theta=u(\cos\theta\cos\delta-\sin\theta\cos\varphi\sin\delta)$$
$$-v_c\cos(\beta+\delta). \quad (25c)$$

Finally, we must solve for $u$ in terms of $\theta$, $\varphi$, $\beta$. This can be done by squaring each of the equations (25) and adding:

$$V_p^2=u^2+v_c^2-2Auv_c, \quad (26)$$
$$A=\sin\theta\cos\varphi\sin\beta+\cos\theta\cos\beta.$$

This quadratic equation can be solved for $u$ to give:

$$u=Av_c+[V_p^2+v_c^2(A^2-1)]^{\frac{1}{2}}, \quad (27)$$

where the nonphysical solution has been discarded.

The Jacobian of the transformation is found from the following identity:

$$\cos\Theta\,\sin\Theta\left(\frac{\partial\Theta}{\partial\theta}\frac{\partial\Phi}{\partial\varphi}-\frac{\partial\Theta}{\partial\varphi}\frac{\partial\Phi}{\partial\theta}\right)$$
$$\equiv\left(\frac{\partial}{\partial\theta}\sin\Theta\,\cos\Phi\right)\left(\frac{\partial}{\partial\varphi}\sin\Theta\,\sin\Phi\right)$$
$$-\left(\frac{\partial}{\partial\varphi}\sin\Theta\,\cos\Phi\right)\left(\frac{\partial}{\partial\theta}\sin\Theta\,\sin\Phi\right).\quad(28)$$

Equation (28) is easily proved by carrying out the differentiations indicated on the right-hand side, collecting terms and simplifying.

Substituting Eqs. (25a) and (25b) into the right-hand side of (28) and dividing through by $V_p\sin\theta$ and $V_p\cos\Theta$ given by Eq. (25c), we get, after much simplification:

$$\frac{\sin\Theta}{\sin\theta}J\begin{pmatrix}\Theta, & \Phi\\ \theta, & \varphi\end{pmatrix}=\frac{u^2}{V_p[V_p^2+v_c^2(A^2-1)]^{\frac{1}{2}}},\quad(29)$$

which is Eq. (6) of the text.

PHYSICAL REVIEW VOLUME 120, NUMBER 5 DECEMBER 1, 1960

# Theoretical Study of the Electron Drift Velocity in Binary Gas Mixtures with Applications to A-$CO_2$ and A-$N_2$ Mixtures*

Martin A. Uman
*Department of Electrical Engineering, Princeton University, Princeton, New Jersey, and Elcon Laboratory, Incorporated, Cambridge, Massachusetts*

AND

George Warfield
*Department of Electrical Engineering, Princeton University, Princeton, New Jersey*

(Received May 17, 1960)

Starting with the Boltzmann equation, a theoretical expression is developed for the electron drift velocity in a binary gas mixture. The theory reduces to that of Morse, Allis, and Lamar in the absence of one of the gases. The theory is applied to pure argon and to mixtures of A–0.1% $CO_2$, A–0.16% $CO_2$, A–1.0% $CO_2$, A–0.1% $N_2$, A–0.5% $N_2$, and A–1.0% $N_2$. The theoretical drift velocity curves for A–$CO_2$ are in close agreement with experimental data, whereas the A–$N_2$ curves differ from experimental data. Possible reasons for this discrepancy are discussed.

## I. INTRODUCTION

SMALL amounts of nitrogen or of carbon dioxide, when added to argon, alter appreciably the value that the electron drift velocity has in pure argon. Experimental studies of A–$CO_2$ mixtures have been performed by English and Hanna[1] and by Errett.[2] Experimental studies of A-$N_2$ mixtures have been performed by Kirshner and Toffollo,[3] Colli and Facchini,[4] Engligh and Hanna,[1] and Errett.[2] "Pure" argon curves, which in reality may be A–$N_2$–? mixtures, have been published by Allen and Rossi,[5] Kelma and Allen,[6] and Hudson.[7] Pure argon has been studied experimentally by Nielsen,[8] Herreng,[9] Colli and Facchini,[4] Kirshner and Toffollo,[3] and Errett;[2] and theoretically by Allen[10] and Bowe.[11]

In this paper a theoretical expression for the electron drift velocity in a binary gas mixture is derived and applied to A–$CO_2$ and A–$N_2$ mixtures. In the limit of one gas the theory accurately predicts the drift velocity curve of pure argon. The agreement between theory and experiment for A–$CO_2$ mixtures is quite good, lending strong support to the theoretical approach. For A–$N_2$ mixtures the theory is not in good agreement with any of the published experimental data. There are, however, significant differences between the experimental data reported by different workers. It is postulated that either (1) the A–$N_2$ mixtures may contain

* This work was supported in part by Avco Corporation, Research and Advanced Development Division, Wilmington, Massachusetts.

[1] W. H. English and G. C. Hanna, Can. J. Phys. **31**, 768 (1935).
[2] D. Errett, doctoral thesis, Purdue University, 1951 (unpublished).
[3] J. M. Kirshner and D. S. Toffollo, J. Appl. Phys. **23**, 594 (1952).
[4] L. Colli and U. Facchini, Rev. Sci. Instr. **23**, 39 (1952).
[5] J. Allen and B. Rossi, PB 50914, Manhattan Engineers District L. A. Report 115—Series B MDDC Report 448, July, 1944 (unpublished).
[6] E. D. Kelma and J. S. Allen, Phys. Rev. **77**, 661 (1950).
[7] D. Hudson, Atomic Energy Commission Report, DDC 524, 1946 (unpublished).
[8] R. A. Nielsen, Phys. Rev. **50**, 950 (1936).
[9] P. Herreng, Compt. rend. **217**, 75 (1943).
[10] Harriet Allen, Phys. Rev. **52**, 707 (1937).
[11] J. C. Bowe, Argonne National Laboratory Report 5967 (unpublished).